Aeromagnetic anomalies and structural model of the Chicxulub multiring impact crater, Yucatan, Mexico

Mario Rebolledo-Vieyra[1], Jaime Urrutia-Fucugauchi[2,*], and Héctor López-Loera[3]

[1] Centro de Investigaciones Científicas de Yucatán, CICY, Centro para el Estudio del Agua, Calle 43 No. 130, Colonia Chuburná de Hidalgo, 97200 Mérida, Yucatán, Mexico.
[2] Universidad Nacional Autónoma de México, Instituto de Geofísica, Proyecto Universitario de Perforaciones en Océanos y Continentes, Circuito Exterior s/n, Cd. Universitaria, Del. Coyoacán, 04510 Mexico D.F., Mexico.
[3] Instituto Potosino de Investigación Científica y Tecnológica, IPICYT, Camino a la Presa San José 2055, Col. Lomas 4a sección, 78216 San Luis Potosí, S.L.P., Mexico.
** juf@geofisica.unam.mx*

ABSTRACT

A structural model of the Chicxulub crater is derived from aeromagnetic anomaly modeling, borehole information and magnetic mineral data. Magnetic susceptibility measurements from borehole cores and samples in the crater show that suevite-like breccias have a variable strong magnetic signature, which is related to basement and melt clasts. The crystalline component estimated from clast analyses in the suevite-like breccias has on average higher magnetic susceptibilities (up to 1200×10^{-5} SI) than that of impact melt (~500×10^{-5} SI) and crystalline basement (400×10^{-5} SI). Reduction to the pole and downward analytical continuations show the discrete composite character of the anomaly, with inverse dipolar anomalies. The second-derivative of magnetic anomaly depicts five concentric rings, with the external ring correlating with the cenote ring and marking the surface expression of crater rim. The analytical signal and the radially averaged spectrum yield an estimate of the averaged depth to the magnetic sources, ranging from 1000 to 6000 m. There are three major magnetic sources within the Chicxulub crater: 1) the melt unit, 2) the suevite-like breccia, and 3) the central uplift. Using all these data, including new 2-D magnetic models, a new structural model is proposed. It reveals a system of regional vertical faults that explain the magnetic signal over the southern sector of the crater, whereas a 2.5 km deep central uplift and highly magnetized breccia sequences and melt sheet might be the sources of the main magnetic anomalies.

Key words: Chicxulub crater, magnetic susceptibility, aeromagnetic anomaly, structural model, uplift, Mexico.

RESUMEN

En este trabajo presentamos un modelo actualizado de la estructura de impacto de Chicxulub, utilizando nuevos modelos de la anomalía aeromagnética. Estudios de la variación de la susceptibilidad magnética a lo largo de la columna litológica al interior del cráter revelan que las brechas de tipo suevita tienen una firma magnética más fuerte que la unidad fundida (melt). La componente cristalina, estimada a partir del análisis de clastos encontrados en las brechas de tipo suevita, tiene una susceptibilidad

Rebolledo-Vieyra, M., Urrutia-Fucugauchi, J., Héctor López-Loera, H., 2010, Aeromagnetic anomalies and structural model of the Chicxulub multiring impact crater, Yucatan, Mexico: Revista Mexicana de Ciencias Geológicas, v. 27, núm. 1, p. 185-195.

magnética más alta (hasta 1200×10^{-5} SI), que el melt (~500×10^{-5} SI) y los clastos del basamento cristalino (400×10^{-5} SI). La reducción al polo y la continuación hacia abajo, documentan el carácter fragmentado de la anomalía. La segunda derivada de la anomalía aeromagnética delinea cinco anillos concéntricos al interior del cráter; el último anillo se correlaciona con el anillo de cenotes, lo cual apoya la interpretación de que el origen del anillo de cenotes está ligado con el cráter. La señal analítica y el espectro radialmente promediado arrojan una profundidad estimada a las fuentes magnéticas que va de los 1000 m a los 6000 m. Utilizando estos datos desarrollamos nuevos modelos magnéticos en 2-D, los cuales indican que el carácter fraccionado en la porción norte del cráter está controlado por un sistema de fallas verticales. La principal anomalía central es producto de un levantamiento estructural, cuya cima se encuentra a ~2,500 m de profundidad a partir del fondo marino, en el área central del cráter.

Palabras clave: cráter Chicxulub, magnetometría, anomalía aeromagnética, modelo estructural, levantamiento, México.

INTRODUCTION

Impact cratering is one of the major processes shaping planetary surfaces in the Solar system. Impact craters are characteristic features in all planets, satellites and asteroids, except for the gaseous giant planets. On Earth, the geological record of impact craters has been erased by the tectonic, magmatic and erosional processes (Melosh, 1989). Large complex multiring craters that are products of major impacts are rare on Earth, with only three craters documented: Vredefort (South Africa), Sudbury (Canada) and Chicxulub (Mexico) (Grieve and Therriault, 2000; Urrutia-Fucugauchi and Perez-Cruz, 2009). Chicxulub is the youngest and best preserved. The impact event is also well known since it has been linked to global effects on climate and environment, resulting in one of the major life turnovers marking the transition from the Mesozoic to the Cenozoic at the Cretaceous/Paleogene (K/Pg) boundary (Hildebrand *et al.*, 1991, 1998; Sharpton *et al.*, 1992).

Geophysical methods have long been used to identify and investigate impact craters, which often show characteristic circular anomaly patterns (*e.g.*, Pilkington and Grieve, 1992; Sharpton *et al.*, 1993). Aeromagnetic and ground magnetic surveys have been particularly successful in studying the structure and stratigraphy of craters. The changes in physical properties induced by shock and pressure/thermal processes have been also studied and related to petrographic and geochemical data and to the impact and cratering processes. Recent investigations on Mars large impact basins, which are characterized by low amplitude magnetic anomalies, indicate apparent major demagnetization effects on target rocks induced by large impacts (*e.g.*, Acuña *et al.*, 1999). These features have been documented by paleomagnetic studies of basement rocks from the Vredefort crater (Muundjua *et al.*, 2007). In general, investigations on terrestrial impact structures and laboratory experiments document wide ranges in magnetic properties (*i.e.*, magnetic susceptibility ranges from diamagnetic range, 0.00 S.I. to 1200×10^{-5} SI). In general, it is considered that the shock produces a drop in the magnetic susceptibility and often in the remanent magnetizations (Plado *et al.*, 1999). Lithologies like the impact melt that cool down slowly may acquire a thermoremanent magnetization (TRM) in the direction of the present magnetic field (*e.g.*, Manicouagan and Chicxulub). In other cases, like in large complex craters, the impact lithologies may acquire a new remanence by reheating and transient stresses; *i.e.*, the thermoremanent and shock remanence (SRM) magnetizations along the direction of the Earth's magnetic field at the time of impact.

Buried in the Yucatan carbonate platform in southeastern Mexico, the Chicxulub crater was unveiled by geophysical surveys conducted as part of oil exploration programs of Pemex (Penfield and Camargo, 1981; Hildebrand *et al.*, 1991; Sharpton *et al.*, 1992). In particular, the buried crater shows a circular concentric Bouguer gravity anomaly pattern, which is clearly marked in the low amplitude regional gravity pattern. The central zone of the gravity anomaly is marked by high amplitude magnetic anomalies. The magnetic anomaly of Chicxulub crater is an example of a complex crater geophysical signature, and in geophysical models, it has a semi-circular shape with a large amplitude central anomaly surrounded by smaller inverse dipolar anomalies (Figure 1). In the past two decades, the crater has been intensively investigated using potential field, electromagnetic and seismic surveys. Although numerous studies and geophysical modeling have been used to investigate the crater structure (*e.g.*, Hildebrand *et al.*, 1991, 1998; Sharpton *et al.*, 1992, 1993; Connors *et al.*, 1996; Morgan *et al.*, 1997; Morgan and Warner, 1999; Delgado-Rodríguez *et al.*, 2001; Gulick *et al.*, 2008; Veermesch and Morgan, 2008), inverse and forward models derived from these data are limited by the lack of direct data on the nature of target lithologies. Data on physical properties of target lithologies and specially of the deep Yucatan basement remain poorly constrained. Stratigraphic data came mainly from oil exploration boreholes and regional models (*e.g.*, Murray and Weide, 1962; López-Ramos, 1973, 1983; Marshall, 1974; Weidie, 1985, Ward *et al.*, 1995). Recent drilling programs that included continuous coring have provided new information on the subsurface stratigraphy and constraints on the basement (Urrutia-Fucugauchi *et al.*, 1996, 2004a, 2008; Rebolledo-

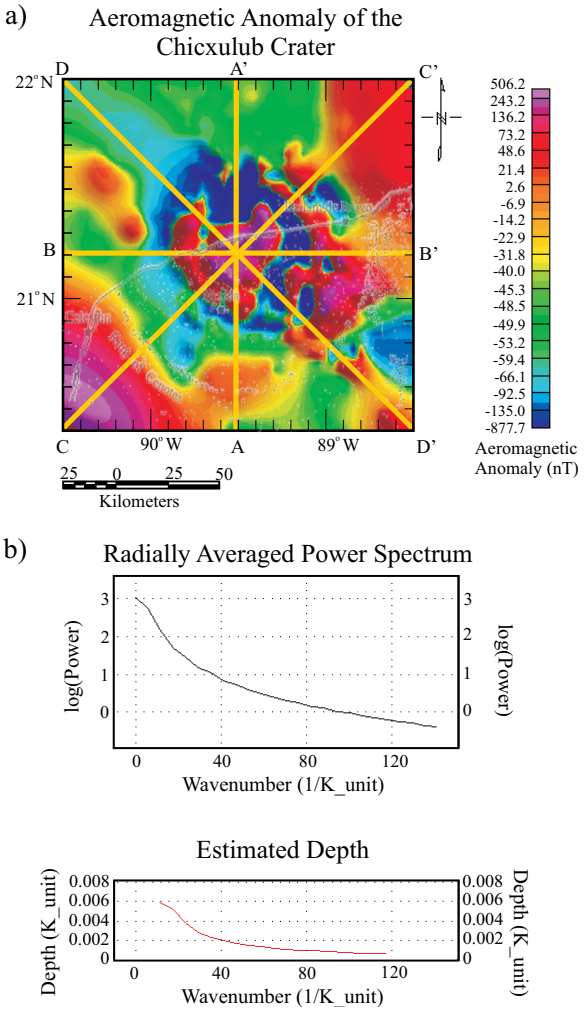

Figure 1. a: Aeromagnetic anomaly field over the Chicxulub crater in the Yucatan peninsula and Gulf of Mexico. Survey flight altitude is 450 m above sea level. Location of regional profiles are shown: Lines A-A', B-B', C-C' and D-D' used for 2-D modeling (see Figures 3 and 4). b: Radially averaged spectra of the aeromagnetic anomaly, units in the vertical axis are depth in km.

Vieyra *et al.*, 2000). Laboratory measurements on physical properties provide data needed to constraint geophysical modeling. Samples from the Chicxulub suevitic breccias and from PEMEX boreholes that provide information on the nature of the Yucatan basement are also considered to constrain the structural crater model.

In this work, we present new structural models of the impact crater derived from modeling of the aeromagnetic anomaly field (Figure 1). In the analysis, we consider previous modeling of the aeromagnetic anomalies (Pilkington *et al.*, 1994; Ortiz-Alemán *et al.*, 2001), borehole and geophysical logging information (Urrutia-Fucugauchi *et al.*, 1996, 2004a, 2008; Rebolledo-Vieyra *et al.*, 2000), paleomagnetic, rock magnetic and geochemical data (Urrutia-Fucugauchi *et al.*, 1994, 1996, 2004b; Urrutia-Fucugauchi and Pérez-Cruz, 2008). First, the magnetic measurements on rock samples are presented. In the following section, the processing and analysis of the aeromagnetic data are analyzed. Then the magnetic modeling method is described, and results are linked with the paleomagnetic data. Finally, we discuss the combined results with regards to the previous models and the geological constraints of the crater basin.

PETROPHYSICAL AND GEOPHYSICAL DATA

Paleomagnetic and rock magnetic measurements

Natural remanent magnetization (NRM) and low-field magnetic susceptibility measurements were performed on core samples from the UNAM Scientific Drilling Program. The NRM intensity and direction (referred to arbitrary azimuth) were determined using a spinner JR-5 magnetometer. The low-field magnetic susceptibility was measured with the Bartington susceptibility system, using the laboratory sensor. We thus obtained high-resolution records of the magnetic susceptibility behavior from three boreholes drilled in the southern sector of the structure (Rebolledo-Vieyra and Urrutia-Fucugauchi, 1999). From these studies we obtained log data of magnetic susceptibility for the suevitic breccias, which have mean magnetic susceptibility of 229×10^{-5} SI, but with values as high as 1200×10^{-5} SI, for bunte breccia with a susceptibility mean within the diamagnetic range, for individual clasts of impact melt, 500×10^{-5} SI, and crystalline basement, 400×10^{-5} SI, and also for the carbonates and anhydrites, which magnetic susceptibility is also within the diamagnetic range. The $^{40}Ar/^{39}Ar$ dates reported by Sharpton *et al.* (1992) on melt samples recovered from the PEMEX borehole Chicxulub-1 give an age for the impact of ~65.5 Ma. The isotopic dates agree with the paleomagnetic data of the melt samples, which place the impact within reverse polarity geomagnetic chron C29r. The magnetic polarity of melt, investigated by Urrutia-Fucugauchi *et al.* (1994) in PEMEX borehole Yucatan-6, Rebolledo-Vieyra and Urrutia-Fucugauchi (2004) in Yaxcopoil-1 borehole, and Rebolledo-Vieyra and Urrutia-Fucugauchi (2006) in UNAM boreholes give reverse polarity, with mean upward inclinations of 40°–42°. Considering this data, we assumed a -41° inclination and a declination of 163° using the North America polar wander curve for the Late Cretaceous-early Paleogene.

Aeromagnetic anomaly data

The aeromagnetic data come from a 450 m flight-altitude survey. Data for the modeling have been reduced to a regular anomaly grid 171 km by 171 km, with digitized data points every 1 km. Data processing consisted in reduction to the pole (Figure 2a), second vertical derivative (Figure 2b), pseudo-gravity (Figure 2c) and analytical downward continuations (Figure 2d); we also calculated the radial

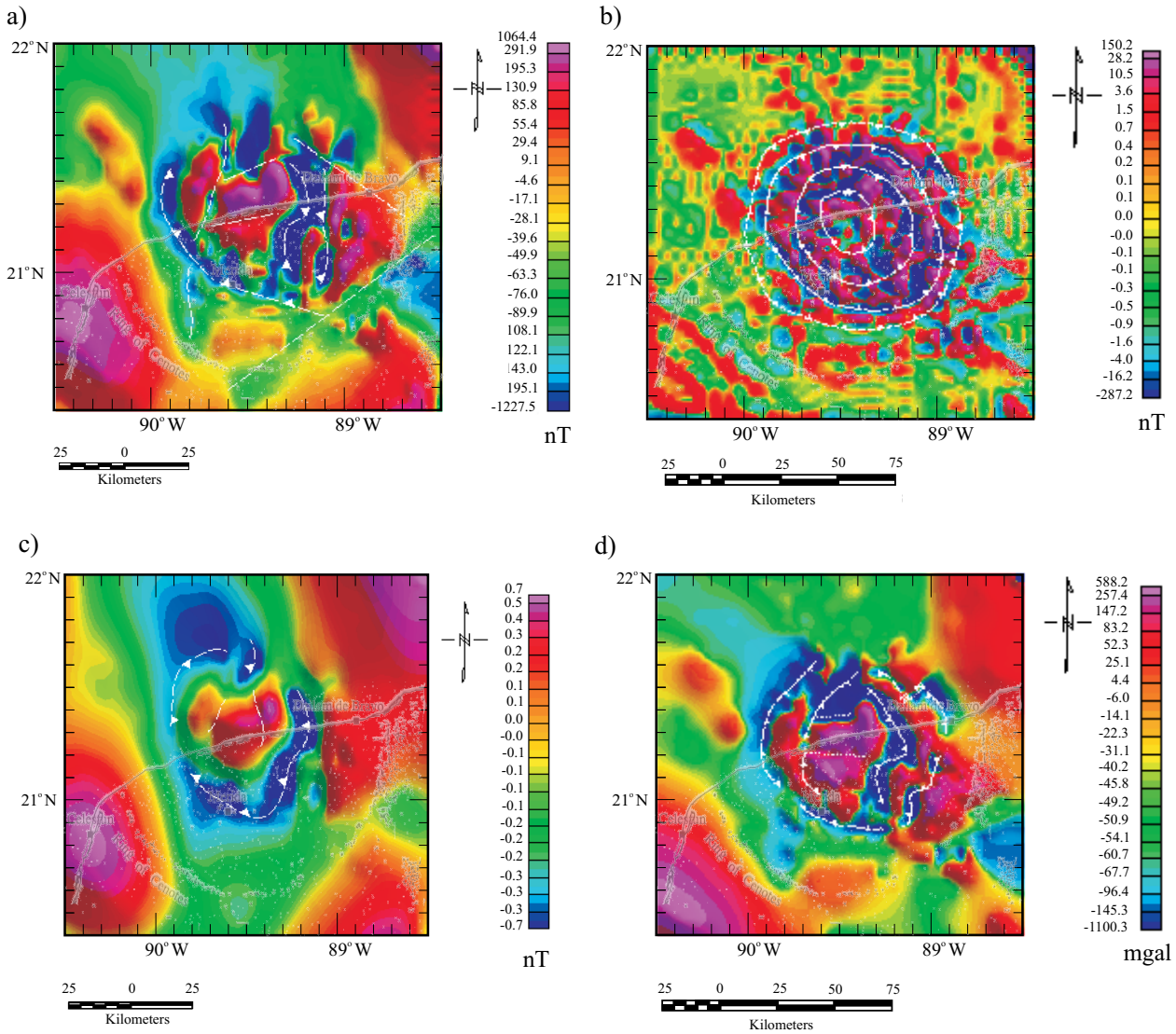

Figure 2. a) Aeromagnetic anomaly field of the Chicxulub crater reduced to magnetic pole. Local geomagnetic field inclination is 45° and declination is 5°. b) Second derivative of the aeromagnetic anomaly field. c) Pseudo-gravimetric analysis of aeromagnetic anomaly field. Density contrast is 1.8 g/cm^3. d) Downward continuation to a reference surface of 450 m.

average spectrum to estimate the depth to sources (Figure 2e) (*e.g.*, Macleod *et al.*, 1993; Pilkington and Hidebrand, 2000). Using this data, we modeled four regional profiles, oriented N-S, E-W, N45°E and N45°W crossing the entire basin (Figure 1). Data processing and modeling was made with the Oasis Montaj software package. From this process, we constrained the principal structures of the crater as being separated into several magnetic domains. In the analysis, we considered a magnetic domain as a region with similar magnetic characteristics in terms of wavelengths and amplitudes. In some cases, low amplitude magnetic anomalies, characterized by subdued signals, and null or weak magnetic susceptibility contrasts have also been separated into distinct domains. When noticeable contrasts in anomaly amplitudes, possibly associated with magnetic susceptibility contrasts, are observable within a domain, we call them magnetic sub-domains (Figure 2).

Analyses of the aeromagnetic anomaly field (Figure 1a) suggest separation of anomaly patterns into three domains, with characteristic amplitudes and wavelengths. The first is characterized by large amplitude dipolar magnetic anomalies located at the central part of the crater, extending onshore and offshore. It has, at least, three magnetic highs, one of them having an isolated maximum and the other two having dipolar high to low distances between 7 and 10 km. Two magnetic sub-domains can be separated: A sub-domain associated with magnetic responses of long wavelengths and large amplitudes, and a second magnetic sub-domain located SE from the first sub-domain and completely onshore. The magnetic configuration of this

anomaly has three anomalous zones, with normal dipolar behavior; the dipolar distances range from 7 to 8 km. This magnetic sub-domain is characterized by anomalies with long wavelengths and intermediate amplitudes. In the total magnetic field anomaly map, this domain has an elongated trend oriented N80°W, with a maximum length of 70 km and 40 km wide. The second aeromagnetic domain is located to the SW, and is characterized by an isolated high anomaly with an oval shape striking NW, defined by long wavelengths and large amplitudes; its minimum dimensions are 64 km, striking NW, and 50 km, striking NE. The third magnetic sub-domain, located to the NE, has an elongated shape with more than 50 km length in either direction. The configuration reflects presence of major lineaments striking NE-SW and NW-SE. Within the magnetic domain zones, secondary lineaments can be observed, and an E-W lineament that apparently limits the magnetic anomaly forming the first magnetic sub-domain; its fragmented character can be associated to faults and/or fractures.

To estimate average statistical depths to magnetic sources, we calculated the radially averaged spectrum (Figure 1b). In the depth estimations, it is assumed that the ejecta blanket within the crater behaves as a coherent and continuous deposit, allowing us to estimate the depth to the sources at about ~6,000 m in the center of the structure to ~500 m towards the edge of the central anomaly.

AEROMAGNETIC DATA PROCESSING AND MODELING

Reduction to magnetic pole

The configuration of the magnetic field reduced to the pole permits separation of three magnetic domains (Figure 2a). The first magnetic domain is located in the central part, and it is formed by four magnetic anomalies with dipolar configurations. The first anomaly is located in the NW within the domain; it is elongated striking NNE and has a polar distance of 17 km and is associated to a magnetic response of short-long wavelengths and intermediate amplitude. The second anomaly is located within the NW central portion of the magnetic domain and is formed by a normal dipolar anomaly, elongated and striking ENE with high-to-low distance of ~17 km. The anomaly consists of two positive highs that in the north, as in the south, present dipolar configuration; to the north it has normal polarity and to the south it has reverse polarity. A ENE-striking lineament that borders the anomaly domain divides the two lobes. These sub-domains present magnetic anomalies of long wavelengths and large amplitudes. The third zone of this magnetic domain is characterized by a normal dipolar anomaly, elongated, striking N-S, with a polar high-to-low distance of about 9 km, associated to a magnetic response of long wavelengths and intermediate amplitudes. The fourth magnetic sub-domain is formed by a triangular shaped anomaly that in its central part shows a normal dipole with a polar high-to-low distance of about 17 km. This sub-domain is characterized by intermediate wavelengths and amplitudes.

The second magnetic domain, located SW from the central zone, is formed by an anomaly with long wavelength and large amplitude. The anomaly has an oval trend with the long axis striking NE-SW, and covers a large area located onshore and offshore.

The third magnetic domain is located NE from the central zone and is characterized by an anomaly associated to a long wavelengths and large amplitude signal. To better constrain the magnetic characteristics of the zone, it is necessary to have a more extensive magnetic coverage.

Lineaments identified in analyses of magnetic anomaly trends support the occurrence of faulting and fracturing at depth. Lineaments striking NW-SE, NE-SW and N-S border the anomaly domain zones. A major lineament striking NNE-SSW crosses the crater basin, separating the anomaly domain zones one and two of the first domain. The dimensions estimated in this analysis for the structure are a maximum longitude of 167 km striking NW76SE and a perpendicular distance of 106 km.

Second vertical derivative

The second vertical derivative yields a magnetic configuration that emphasizes the circular trends in the magnetic anomaly field (Figure 2b). Three circular trends are unveiled. The first is formed by an interior ring of 71.5 km striking NW and 65.5 km striking NE. The second is associated to a circular intermediate ring with a longitude of 137 km striking NW and 113 km in the NE direction. The third trend is poorly defined.

Pseudo-gravimetry

The pseudo-gravimetric anomaly, which is the vertical derivative of the pole-reduced magnetic potential, was calculated. With this analysis (Figure 2c) four domains are identified: the central larger domain may correspond to a broad low, separated by a high in the middle. The other three pseudo-gravimetric domains are located on the flanks of the broad low, and are represented by the pseudo-gravimetric highs at W, SW, SE, E and NE. Within this pseudo-gravimetric configuration, the main lineaments are observed striking NNW-SSE and ENE-WSW.

Downward analytical continuations

Downward analytical continuations of the aeromagnetic anomaly were computed down to a reference surface 450 m depth (Figure 2d). Results of this analysis showed

that the reduced anomaly field is composed by a series of dipolar and isolated high/low magnetic anomalies, which can be grouped in three magnetic domains. The first and main domain is located in the central part of the configuration and is conformed by two magnetic sub-domains. The first presents a magnetic anomaly characterized by three positive lobes with two of normal polarity associated to magnetic responses with long wavelengths and large amplitudes. The second sub-domain is located to the SE and is characterized by intermediate to short long wavelength with medium amplitudes. The second lobe is located to the SE from the first sub-domain and is characterized by intermediate longitude and amplitude wavelengths. The second domain is located to the SW from the center and characterized by a dipolar anomaly of large dimensions elongated with a NW-SE trend. This lobe, though poorly defined is formed by long wavelengths and large amplitudes. The third magnetic domain is located to the N, NW and NE from the center of the configuration, it has an inverted-U shape and long wavelengths and large amplitudes. At its W limit, it has a large magnetic high with isolated highs and lows. This domain has large dimensions and it surrounds the central magnetic domain towards its limits NW, N and NE. Analysis of the downward continuation field shows an anomalous zone of 161 km long, striking NW and 143 km in the NE direction.

Two-dimensional modeling

To further constrain the geometry and relative location of source bodies, forward two-dimensional models along regional profiles crossing the basin were constructed. The profiles are oriented N-S (A-A' profile; Figure 1a), E-W (B-B' profile; Figure 1a), N45°E (C-C' profile; Figure 1a) and N45°W (D-D' profile; Figure 1a).

N-S profile (Figure 1a, A-A'; Figure 3a) shows a magnetic high towards the center of the profile, ~20 km in width; the "pick to pick" magnetic range is ~700 nT. From the profile, and the aeromagnetic anomaly, the central magnetic anomaly is fragmented and it might be associated to a fault system. This central magnetic high is associated with the central basement uplift in complex crater models (Melosh, 1989; O´Keefe and Ahrens, 1999). The basement material is highly magnetic. The depth to the top of the central uplift is estimated from our models to be from 2000 to 2900 m. The top of the central uplift is tilted rather than flat, capped by a ~400 m thick cover of impact lithologies. The central uplift is bounded by two mayor lineaments and it shows an important lineament at the top of the central anomaly and a series of smaller lineaments towards the northern limit, which account for the irregular behavior of the magnetic low. We inferred that these lineaments might be associated to faulting or fractures. Towards the south of the profile, where the CSDP Yaxcopoil-1 borehole is located at about 62 km from the crater center, we found a magnetic high that is probably associated with impact lithologies at ~1000 depth and an approximate thickness of 1000 m.

E-W profile (Figure 1a, B-B'; Figure 3b). In this model, as in the N-S model, the depth to the top of the central uplift is estimated between 2000 and 3000 m. The central uplift is capped by ~400 thick cover of impact lithologies. A striking feature in this model is the high frequency contents along the magnetic profile. The short wavelengths could be associated to shallower magnetic sources or to effects of a fault system located preferentially toward the east of the central uplift. The fault system is characterized by normal faulting based in the high angle and the distribution of the hanging walls. As in the prior models, we considered the suevite-like breccia as the major magnetic source, besides being the shallower source.

N45°W profile (Figure 1a, C-C'; Figure 4a). Faulting towards the northern sector of the profile is incorporated into the model, with a major vertical fault delimiting the central uplift, followed by a series of smaller length vertical faults. In this model, a vertical fault within the top of the central uplift is added. Similar to the characteristics along the N-S profile, there is a large amplitude magnetic high towards the southern portion of the profile (>320 nT). The central large amplitude anomaly is modeled with a body a radius of ~45 km.

N45°E profile (Figure 1a, D-D'; Figure 4b). Model for this profile delineates a major fault zone located towards the northern portion of the crater. The model includes an extensive fault system of high angle dipping normal faults. In the model, a vertical fault is included within the top part of the central uplift. Top of the central uplift is estimated to lie between 2000 and 3000 m.

DISCUSSION

Early geophysical models of the Chicxulub crater have been limited by lack of direct laboratory data on basement, target, impact and crater in-fill Tertiary lithologies. Preliminary data from PEMEX boreholes were incorporated in previous studies (Pilkington *et al.*, 1994, 2000; Urrutia-Fucugauchi *et al.*, 1996; Ortíz-Alemán *et al.*, 2001). There are three major magnetic sources within the Chicxulub crater: 1) the melt unit, 2) the suevite-like breccia, and 3) the central uplift. In this work, magnetic properties of the target and impact lithologies coming from core samples in the UNAM and Chicxulub Scientific Drilling Programs were used to construct structural models and interpretations of the aeromagnetic anomalies. The models presented incorporate the magnetic data obtained from the UNAM boreholes and also the information from prior models. In the radially averaged spectrum, we estimate a depth of ~1000 m to the top of the impact lithologies in the central portion of the anomaly and ~2500 m to the top of the central uplift. From the models, we estimated the thickness and distribution of the impact lithologies. The data obtained from these

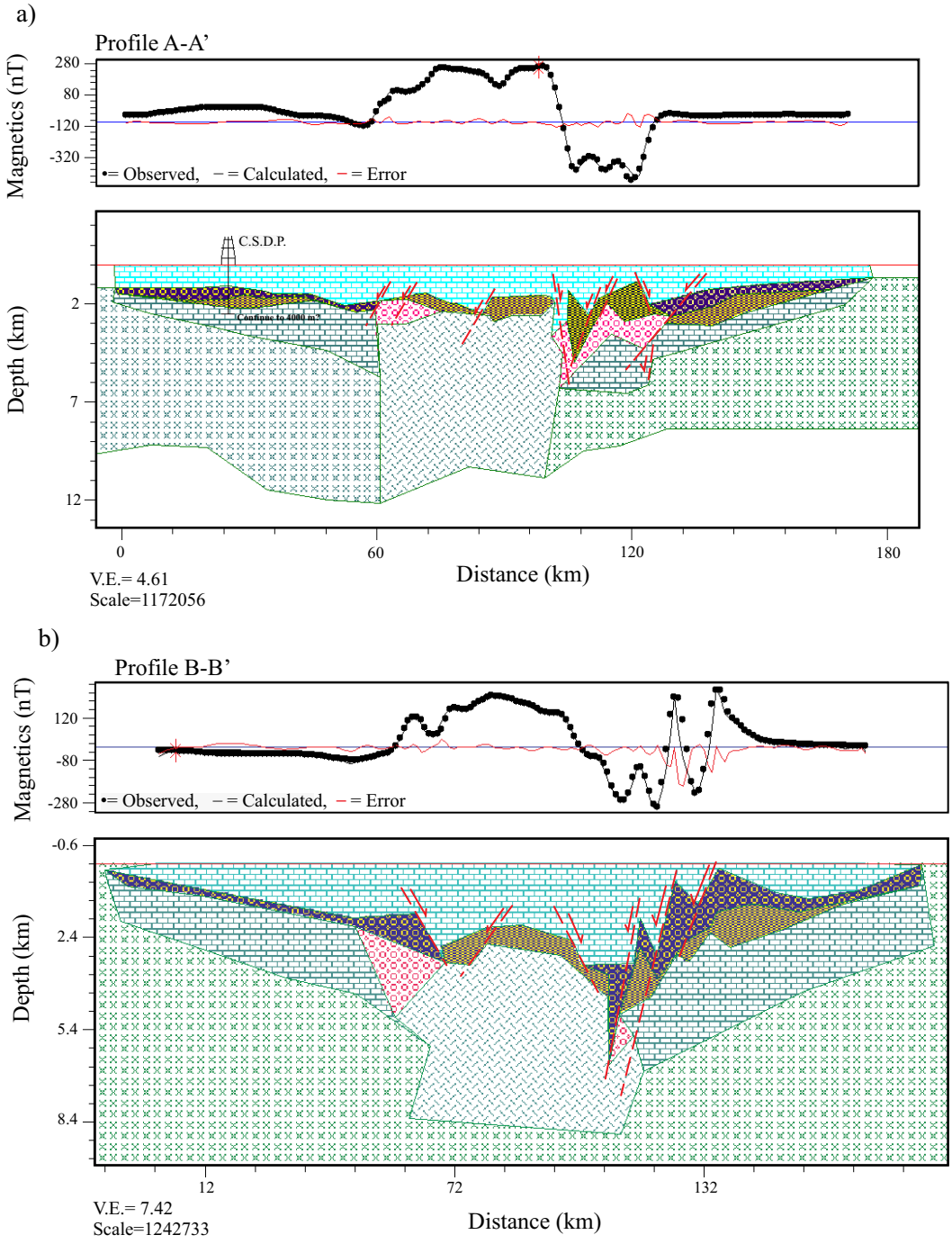

Figure 3. Magnetic models for Chicxulub crater. a) 2-D model of the profile A-A' in Figure 1. b) 2-D model of the profile B-B' in Figure 1.

models document the presence of a fault system towards the central portion of the crater, which is reflected in the magnetic high and lows of the anomaly; this fault system is predicted in the models of formation and evolution of complex-craters. These characteristics are also evident by the analyses performed to the aeromagnetic anomaly, like the downward continuation and the reduction to pole. The circular shape of the central aeromagnetic anomaly is emphasized in the second derivative analysis. The bunte-like breccia and the mega-breccia do not yield a magnetic signal because of the nature of their components, mainly carbonates and evaporites, which are within the diamagnetic range. These characteristics prevented us from having more realistic geological models, even though we have estimated

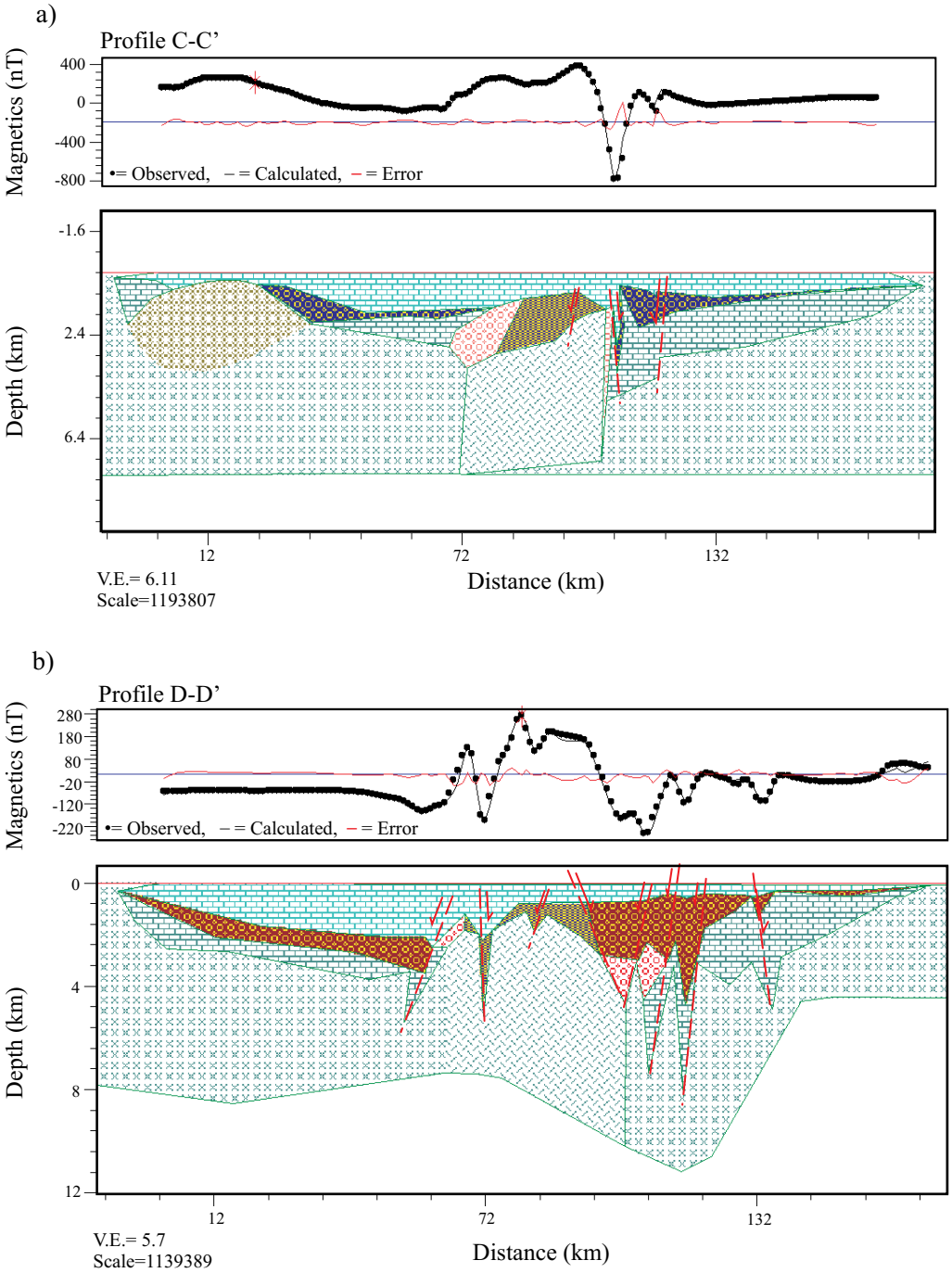

Figure 4. Magnetic models for Chicxulub crater. A) 2-D model of the profile C-C' in Figure 1. B) 2-D model of the profile D-D' in Figure 1.

the depths and thickness of the magnetic sources that, as expected, are thicker towards the center of the structure; however, in places such as in southern portion of the profile A-A', apparent patches of impactite lithologies as thick as 1000 m may be present. From prior drilling experience, we know that in the sequence of impact breccia the suevite-like breccia overlies the bunte-like breccia. We estimate the thickness of the suevite-like breccia to be somewhere between 400 m and 1000 m, but since the bunte-like breccia does not yield a magnetic signal, we assumed that the thickness proposed for the suevite-like includes the bunte-like breccia. Further studies from the CSDP will help solve the problem of the spatial variation of breccia sequence thickness. Recent data from Yaxcopoil-1 borehole does not fit with this interpretation; the Yaxcopoil-1 column documented a 100 m thick impact sequence and no bunte-

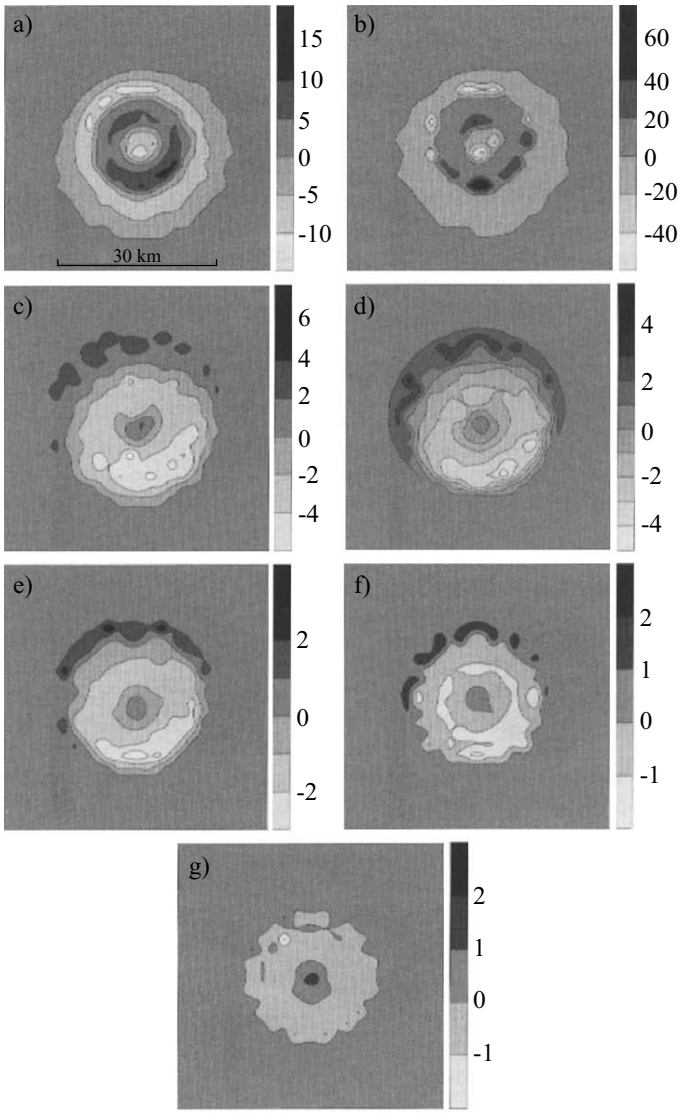

Figure 5 Schematic plan view of the magnetic anomalies (total intensity, nT) of (a) early post-impact, at various erosion levels: (b) 1 km; (c) 2 km; (d) 3 km; (e) 4 km; (f) 5 km; and (g) 6 km. The impact took place at center of the area. Note that the amplitude scale varies.

like breccia underlying the suevite-like breccia (Kring *et al.*, 2004; Urrutia-Fucugauchi *et al.* 2004a, 2004b). However, Yaxcopoil-1 borehole may have been drilled in the terrace zone close to a fault where impact lithologies pinch-out, with the result of thinner impact sequence than expected and thus the lithological sequence recovered might not be representative of the southern crater sector. Total field magnetic anomalies are calculated at various levels using a simple structural model for the central crater structure, assuming the major magnetic source bodies. Results are summarized in Figure 5, from ground surface to a 6 km level reference surface. Taking into consideration the spatial and frequency characteristics of the aeromagnetic anomaly and the borehole information we submit that the geophysical models presented in this study are well supported and represent the structure in the central-southern crater sector.

CONCLUSIONS

There are three major magnetic sources within the Chicxulub crater: 1) the melt unit, 2) the suevite-like breccia, and 3) the central uplift. Reduction to the pole and downward analytical continuations show the discrete composite character of the anomaly field, with large amplitude inverse dipolar anomalies in the central sector. The second-derivative of the magnetic anomaly depicts five concentric rings with the external ring correlating with the cenote ring. The analytical signal and the radially averaged spectrum yield

an estimate of the depth to the magnetic sources that ranges from 1000 to 6000 m. From the radially averaged spectrum we estimate a depth of ~1000 m to the top of the impact lithologies in the central portion of the anomaly and ~2500 m to the top of the central basement uplift. From the models we estimate the thickness and distribution of the impact breccia sequence and melt sheet. The 2-D models document the presence of a fault system towards the central portion of the crater, which is reflected in the magnetic high and lows of the aeromagnetic anomalies; this fault system is predicted in structural models of formation and evolution of complex multiring craters. These characteristics are also evident by the analyses performed to the aeromagnetic anomaly, like the downward continuation and the reduction to pole. The second derivative maps emphasize the circular shape of the aeromagnetic high amplitude anomaly.

Using all these data, including new 2-D magnetic models, a new structural model is proposed, which reveals a system of regional high-angle faults that explain the magnetic signal over the southern sector of the crater, whereas a 2.5 km deep central uplift and highly magnetized breccia sequences and the melt sheet might be the sources of the main magnetic anomalies.

ACKNOWLEDGMENTS

This study forms part of the Research Program on Chicxulub Crater and the UNAM Scientific Drilling Program on Continents and Oceans. Comments by two journal reviewers on an early version of the paper are greatly acknowledged. Thanks to Adrien LeCossec for assistance with preparation of the manuscript figures. Partial financial support for the study has been provided by DGAPA PAPIIT Project IN-114709, CONACYT 224932 and the Ixtli Digital Observatory Project.

REFERENCES

Acuña, M., Connernney, J., Ness, N.F., Lin, R., Mitchell, D., Carlson, C., McFadden, J., Anderson, K., Reme, H., Mazelle, C., Vignes, D., Wasilewski, P., Clouthier, P., 1999, Global distribution of crustal magnetization discovered by the Mars Global Surveyor MAG/ER experiment: Science, 284, 790-793.

Connors, M., Hildebrand, A.R., Pilkington, M., Ortiz-Aleman, C., Chavez, R.E., Urrutia-Fucugauchi, J., Graniel-Castro, E., Camara-Zi, A., Vasquez, J., Halpenny, J.F., 1996, Yucatan karst features and the size of Chicxulub crater: Geophysical Journal International, 127, F11-F14.

Delgado-Rodríguez, O., Campos-Enríquez, J.O., Urrutia-Fucugauchi, J., Arzate, A., 2001, Occam and Bostick 1-D inversion of magnetotelluric soundings in the Chicxulub impact crater, Yucatan, Mexico: Geofisica Internacional, 40, 271-283.

Grieve, R.A.F., Therriault, A., 2000, Vredefort, Sudbury, Chicxulub: Three of a kind: Annual Reviews Earth Planetary Sciences, 28, 305-338.

Gulick, S., Barton, P., Christeson, G., Morgan, J., MacDonald, M., Mendoza-Cervantes, K., Urrutia-Fucugauchi, J., Vermeesch, P., Warner, M., 2008, Importance of pre-impact crustal structure for the asymmetry of the Chicxulub impact crater: Nature Geoscience, 1, 131-135

Hildebrand, A.R., Penfield, G.T., Kring, D.A., Pilkington, M., Camargo, A., Jacobsen, S.B., Boyton, W.B., 1991, Chicxulub Crater: A possible Cretaceous/Tertiary boundary impact crater on the Yucatan Peninsula, Mexico: Geology, 19, 867-871.

Hildebrand, A.R., Pilkington, M., Ortiz-Aleman, C., Chavez, R.E., Urrutia-Fucugauchi, J., Connors, M., Graniel-Castro, E., Niehaus, D., 1998, Mapping Chicxulub crater structure with gravity and seismic reflection data *in* M.M. Graddy, R. Hutchinson, G.J.H. McCall, D.A. Rotherby (eds), Meteorites: Flux with Time and Impact Effects: Geological Society Special Publication, 140, 153-173.

Kring, D.A., Horz, L., Zurcher, L., Urrutia-Fucugauchi, J., 2004, Impact lithologies and their emplacement in the Chicxulub impact crater: Initial results from the Chicxulub scientific drilling project, Yaxcopoil, Mexico: Meteoritics and Planetary Science, 39, 879-897.

López-Ramos, E., 1973, Estudio geológico de la península de Yucatán: Boletín de la Asociación Mexicana de Geólogos Petroleros, 25: 23-76.

López-Ramos, E., 1983, Geología de México: México, D.F., Universidad Nacional Autónoma de México, 3a. ed., 453 pp.

MacLeod, I.N., Vieira, S., Chaves, A.C., 1993, Analytic signal and reduction-to-the-pole in the interpretation of total magnetic field data at low magnetic latitudes, *in* Proceedings of the 3rd International Congress of the Brazilian Society of Geophysics, 830-835.

Marshall, R.H., 1974, Petrology of subsurface Mesozoic rocks of the Yucatan Platform, Mexico: New Orleans, Lousiana, University of New Orleans, M.S. Thesis, 97 pp.

Melosh, H.J., 1989, Impact Cratering: A Geologic Process: New York, U.S.A., Oxford University Press, 254 pp.

Morgan, J., Warner, M., 1999, Chicxulub: The third dimension of a multiring basin: Geology, 27, 407-410.

Morgan, J., Warner, M., the Chicxulub Working Group, 1997, Size and morphology of the Chicxulub impact crater: Nature, 390, 472-476.

Murray, G.E., Weidie, A.E., 1962, Regional geologic summary of Yucatan Peninsula, *in* Field trip to peninsula of Yucatan: New Orleans, Louisiana, New Orleans Geological Society, 142 pp.

Muundjua, M., Hart, R.J., Gilder, S.A., Carporzen, L., Galdeano, A., 2007, Magnetic imaging of the Vredfort impact crater, South Africa: Earth Planetary Science Letters, 261, 456-468.

O'Keefe, J.D., Ahrens, T.J. ,1999, Complex craters: Relationship of stratigraphy and rings to impact conditions: Journal of Geophysisical Research, 104, 27,091-27,104.

Ortiz-Alemán, C., Urrutia-Fucugauchi, J. Pilkington, M., 2001, Three-dimensional modeling of aeromagnetic anomalies over the Chicxulub crater, *in* Lunar Planetary Science Conference, CD Expanded Abstract Volume: Houston, Lunar and Planetary Institute (LPI) Contribution, abstract no.1962.

Penfield, G.T., Camargo, A., 1981, Definition of a major igneous zone in the central Yucatan platform with aeromagnetics and gravity (abstract), *in* 51st Society Exploration Geophysicists Annual Meeting, Technical Program Abstracts, p. 37.

Pilkington, M., Grieve, R.A.F., 1992, The geophysical signature of terrestrial impact craters: Reviews of Geophysics, 30, 161-181.

Pilkington, M., Hildebrand, A., 2000, Three-dimensional magnetic imaging of the Chicxulub Crater: Journal of Geophysical Research, 105: 23,479-23,491.

Pilkington, M., Hildebrand, A.R., Ortiz-Aleman, C., 1994, Gravity and magnetic field modeling and structure of the Chicxulub crater, Mexico: Journal of Geophysical Research, 99, 13,147-13,162.

Plado, J., Pesonen, L.J. Puura, V., 1999, Effect of erosion on gravity and magnetic signatures of complex impact structures: Geophysical modeling and applications, *in* Dressler, B.O.,Sharpton, V.L. (eds.), Large Meteorite Impacts and Planetary Evolution II: Geological Society of America, Special Paper 339, 229-240.

Rebolledo-Vieyra, M., Urrutia-Fucugauchi, J., 1999, High-resolution magnetic susceptibility record of the impact lithologies of the Chicxulub impact crater: American Geophysical Union Fall

Meeting, San Francisco, California: EOS, Transactions, 80(46), F595.

Rebolledo, M., Urrutia Fucugauchi, J., 2004, Magnetostratigraphy of the impact breccias and post-impact carbonates from borehole Yaxcopoil-1, Chicxulub impact crater, Yucatan, Mexico: Meteoritics and Planetary Sciences, 39, 821-830.

Rebolledo-Vieyra, M., Urrutia-Fucugauchi, J., 2006, Magnetostratigraphy of the Cretaceous/Tertiary boundary and early Paleocene sedimentary sequence from the Chicxulub impact crater: Earth Planets and Space, 58, 1309-1314

Rebolledo-Vieyra, M., Urrutia-Fucugauchi, J., Trejo-Garcia, A., Marin, L., Sharpton, V., Soler, A., 2000, UNAM's Scientific Shallow Drilling Program into the Chicxulub impact crater: International Geology Review, 42, 928-940.

Sharpton, V.L., Dalrymple, G.B., Marín, L., Ryder, G., Shuraytz, B., Urrutia-Fucugauchi, J., 1992, New links between the Chicxulub impact structure and the Cretaceous/Tertiary boundary: Nature, 359, 819-821.

Sharpton, V.L., Burke, K., Camargo-Zanoguera, A., Hall, S., Lee, S.A., Marín, L.E., Suárez-Reynoso, G., Quezada-Muñeton, J.M., Spudis, P.D., Urrutia-Fucugauchi, J., 1993, Chicxulub multiring impact basin: Size and other characteristics derived from gravity analysis: Science, 261: 1564-1567.

Urrutia-Fucugauchi, J., Pérez-Cruz, L., 2008, Post-impact carbonate deposition in the Chicxulub impact crater region, Yucatan platform, Mexico: Current Science, 95, 241-252.

Urrutia-Fucugauchi, J., Perez-Cruz, L., 2009, Multiring-forming large bolide impacts and evolution of planetary surfaces: International Geology Review, 51, 1079-1102.

Urrutia-Fucugauchi, J., Marín, L., Sharpton, V., 1994, Reverse polarity magnetized melt rocks from the KT Chicxulub structure, Yucatan peninsula, Mexico: Tectonophysics, 237, 105-112.

Urrutia-Fucugauchi J., Marin, L., Trejo-Garcia, A., 1996, UNAM Scientific drilling program of Chicxulub impact structure. Evidence for a 300 kilometer crater diameter: Geophysical Research Letters, 23, 1565-1568.

Urrutia-Fucugauchi, J., Morgan, J., Stoeffler, D., Claeys, P., 2004a, The Chicxulub Scientific Drilling Project: Meteoritics and Planetary Science, 39, 787-790.

Urrutia-Fucugauchi, J., Soler, A.M., Rebolledo-Vieyra, M., Vera-Sánchez, P., 2004b, Paleomagnetic and rock magnetic study of the Yaxcopoil-1 impact breccia sequence, Chicxulub impact crater, Mexico: Meteoritics and Planetary Science, 39, 843-856.

Urrutia-Fucugauchi, J., Chavez-Aguirre, J.M., Pérez-Cruz, L., de la Rosa, J.L., 2008, Impact ejecta and carbonate sequence in the eastern sector of Chicxulub crater: Comptes Rendus Geosciences, 341, 801-810.

Veermesch, P.M., Morgan, J., 2008, Structural uplift beneath the Chicxulub impact structure: Journal of Geophysical Research, 113 (B7), B07 103.

Ward W.C., Keller, G., Stinnesbeck, W., Adatte, T., 1995, Yucatan subsurface stratigraphy: Implications and constraints for the Chicxulub impact: Geology, 23, 873-876.

Weidie, A.E., 1985, Geology of the Yucatan Platform, Part I, *in* Ward, W. C., Weidie, A.E., Back, W. (eds.), Geology and hydrology of the Yucatan and Quaternary geology of northeastern Yucatan Peninsula: New Orleans, Louisiana, New Orleans Geological Society, 1-19.

Manuscrip received: February 12, 2008
Corrected manuscript received: August 12, 2009
Manuscript accepted: November 23, 2009